Electronic Supplementary Material (ESI) for Journal of Materials Chemistry C.

Supporting Information

Excitonic recombination dynamics mediated by polymorph transformation in cadmium sulfide nanocrystals

Pan Wang,[a] Zhifang Li,[a] Tianye Yang,[a] Zhiyang Wang,[b] Pinwen Zhu[a] and Mingzhe Zhang[a]*

[a]*State key laboratory of Superhard materials, Jilin University, Changchun 130012, P. R. China.*

[b]*School of Science, Changchun University of Science and Technology, Changchun 130022, China.*

**Corresponding author: Mingzhe Zhang (zhangmz@jlu.edu.cn)*

1. High pressure and high temperature synthesis method

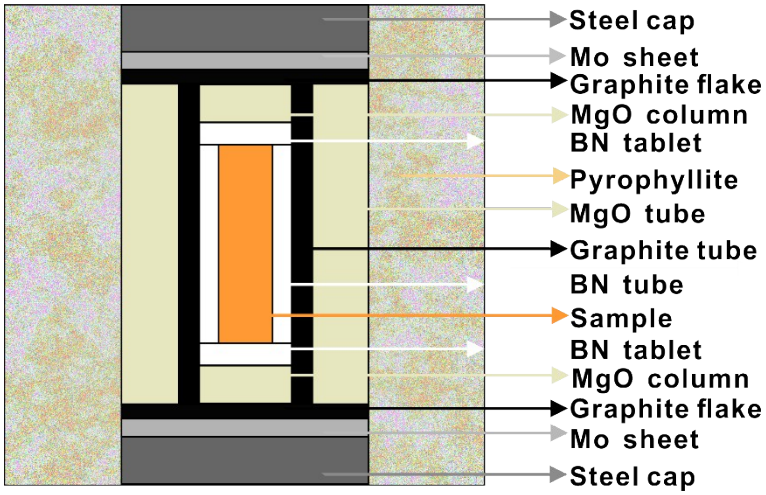

Fig. S1 Schematic illustration of longitudinal section of the cell assembly.

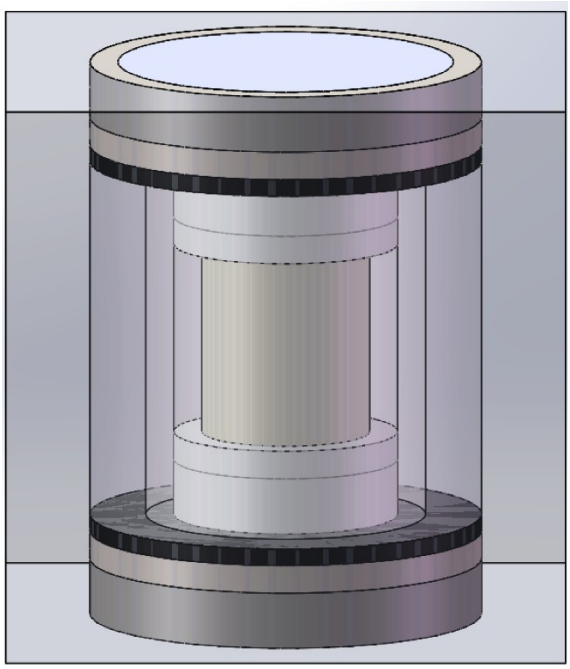

Fig. S2 Three dimensional schematic illustration of an assembled cell.

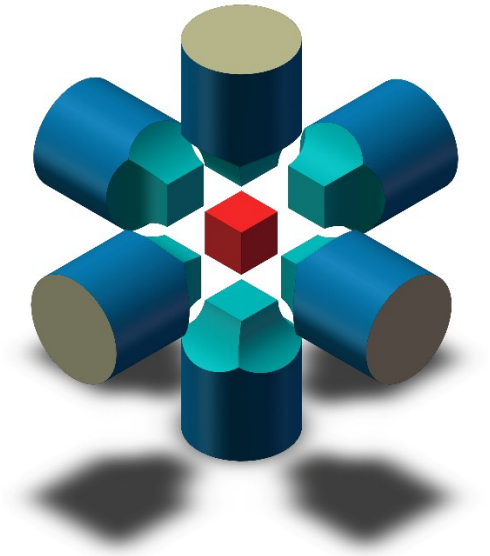

Fig. S3 Schematic illustration of an assembled cell inside the cubic anvil apparatus.

2. Transmission electron microscopy (TEM) images of CdS polymorph

Fig. S4 presents the TEM image of wurtzite starting material, and the recovered zinc-blende and rock-salt CdS polymorphs. As shown in high-resolution TEM (HRTEM) image (Fig. S4b) of the statring material, the measured interplanar spacings of 0.189, 0.316 and 0.336 nm are consistent with (103), (101) and (002) lattice planes of the wurtzite CdS, respectively, in agreement with the selected-area electron diffraction (SAED) images (Fig. S4a). The particle size of the wurtzite starting material

can be clearly distinguished and the average size is 8-10 nm (Fig. S4b). As the synthesis temperature is 150 °C and the pressure is 5.2 GPa, all the diffraction rings (Fig. S4c) of the recovered sample are ascribed to the pure zinc-blende CdS structure with no impurity phases. The measured interplanar spacing (Fig. S4d) of 0.333 nm is a little less than 0.336 nm of (111) lattice planes of the zinc-blende CdS structure, and the observed average particle size is about 8-10 nm. When the synthesis temperature is raised to 300 °C and the pressure remains 5.2 GPa, the recovered sample maintains the pure rock-salt CdS structure, as revealed in TEM images (Fig. S4(e-f)). The measured interplanar spacings (Fig. S4f) of 0.313 nm and 0.314 nm are a little less than 0.316 nm of (111) lattice planes of the rock-salt CdS structure, and the observed average particles size is about 8-10 nm.

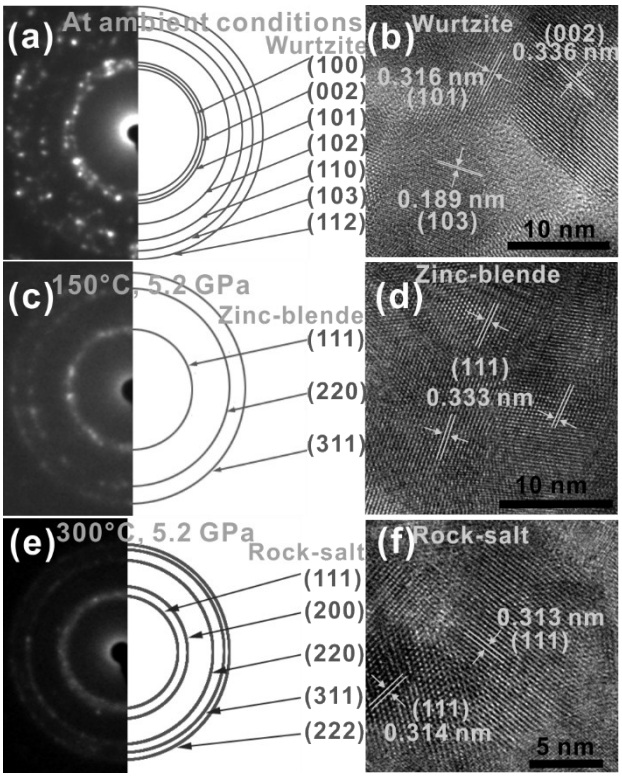

Fig. S4 TEM images of CdS polymorphs. SAED patterns (a), (c) and (e), HRTEM images (b), (d) and (f), correspond to the wurtzite starting material, the recovered zinc-blende sample synthesized by the wurtzite starting material under 5.2 GPa and 150 °C, and the recovered rock-salt sample fabricated by the wurtzite starting material under 5.2 GPa and 300 °C, separately.

3. The electronic structures of three CdS polymorphs

As displayed in Table S1-S3 of energy-dispersive X-ray spectroscopy (EDS) analysis of supporting information, the Cd atomic concentrations are 49.30, 47.37 and 48.01, which are less than the corresponding S atomic concentrations of 50.70, 52.63 and 51.99 for the wurtzite, zinc-blende and rock-salt CdS samples, respectively, indicating the existence of defects such as Cd vacancy, S antisite and S interstitial defects.[1] Moreover, the ratios between the Cd and S atomic concentrations for wurtzite, zinc-blende and rock-salt CdS:Y samples are 0.97, 0.90 and 0.92, separately, suggesting that the high pressure and temperature treatment is in favor of the formation of defects, because the high pressure can compress the crystal lattice to rearrange the atoms and the high temperature can enhance the atomic thermal vibration.[2]

Table S1. Element content percentage of the wurtzite CdS nanocrystals.

Element	Weight (%)	Atom (%)
S	22.68	50.70
Cd	77.32	49.30
Total	100.00	100.00

Table S2. Element content percentage of the zinc-blende CdS nanocrystals.

Element	Weight (%)	Atom (%)
S	24.03	52.63
Cd	75.97	47.37
Total	100.00	100.00

Table S3. Element content percentage of the rock-salt CdS nanocrystals.

Element	Weight (%)	Atom (%)
S	23.56	51.99
Cd	76.44	48.01
Total	100.00	100.00

4. The electronic structures of three CdS polymorphs

The band structures of the three CdS polymorphs along the highly symmetrical k-points directions illustrate the electronic characteristics of the CdS polymorphs (Fig. S5) to better understand the related excitonic recombination dynamics. For the both wurtzite and zinc-blende CdS polymorphs (Fig. S5a and b), the top edges of the valence bands are two-band degenerate and located in the zone centers (G-points), which derive primarily from the S-3p orbits. The bottom edges of the conduction bands for the above both structures (Fig. S5a and b) are also located at G-points, mainly consisting from the hybridized Cd-5s and S-3p orbits. Therefore, both of the wurtzite and zinc-blende CdS structures are direct bandgap semiconductors. Whereas, for the rock-salt CdS structure (Fig. S5c), the top edge of the valence band is located at between X and U point with two-band degenerate, which primarily comes from the S-3p orbits. The bottom edge of the conduction band is located at the different wave vector-X point, which mainly results from the hybridized Cd-5s and S-3p orbits. Hence the rock-salt CdS structure is an indirect bandgap semiconductor, which suggests that the exciton recombination is an indirect transition.

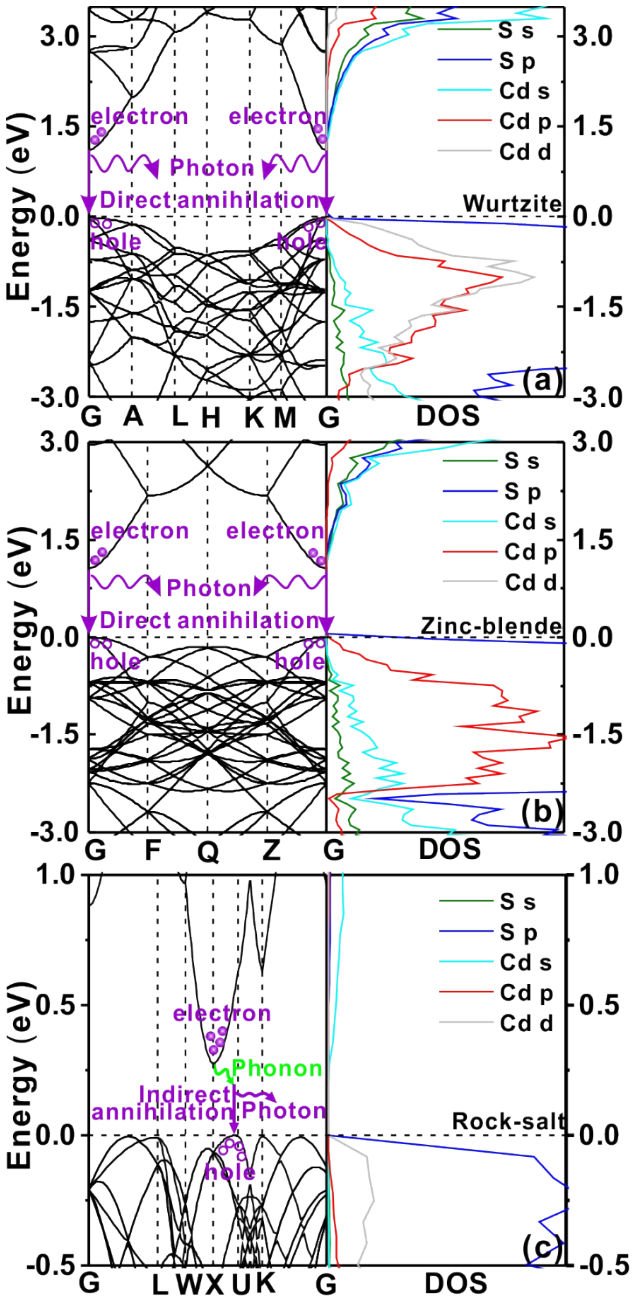

Fig. S5 Schematic illustration of exciton recombination process in a (a) direct and (b) indirect bandgap semiconductor. The energy band structures and exciton recombination processes (left panel), and corresponding density of states (right panel) of (a) wurtzite, (b) zinc-blende, (c) rock-salt CdS polymorphs. The zero of energy is at the Fermi level E_F.

5. The details of constructing the wave functions

The overlap between the electron and hole wave functions is investigated in the wurtzite and zinc-blende CdS polymorphs. The electron and hole wave functions corresponding to the wave functions

of the bottom of the conduction band and the top of the valence band are calculated based on DFT (density-functional theory) calculations using VASP code (Vienna Ab-initio Simulation Package), respectively. In the DFT calculations, the wave functions of the relevant bands in the form of plane waves (coefficients and wave vectors) are stored in the WAVECAR file. The WaveTrans program can read the WAVECAR file, and output a GCOEFF.txt file. The GCOEFF.txt file contains, for each wave vector $\vec{k}$, and band v, a set of $\vec{G}$ values, and corresponding complex plane-wave coefficients $C_{v,\vec{G}}(\vec{k})$, from which the real-space wave functions can be constructed,[3,4]

$$\Psi_{v,\vec{k}}(r) = \sum_{\vec{G}} \frac{C_{v,\vec{G}}}{\sqrt{V}} e^{i(\vec{k}+\vec{G})\cdot\vec{r}} = \sum_{G_x,G_y,G_z} \frac{C_{v,\vec{G}}}{\sqrt{V}} e^{i[(k_x+G_x)x+(k_y+G_y)y+(k_z+G_z)z]} \quad (1)$$

V is the volume of a unit cell (included for normalization purposes). The ϕ_{xy}, ϕ_{yz} and ϕ_{xz} denoted as the xy, yz and xz planar components of total wave functions Ψ_{xyz} are displayed (Fig. S1 and Fig. 4) to provide an intuitive understanding of the wave functions for wurtzite and zinc-blende CdS structures, respectively.

$$\phi_{xy} = \sum_{G_x,G_y} \frac{C_{v,\vec{G}}}{\sqrt{V}} e^{i[(k_x+G_x)x+(k_y+G_y)y]} \quad (2)$$

$$\phi_{yz} = \sum_{G_y,G_z} \frac{C_{v,\vec{G}}}{\sqrt{V}} e^{i[(k_y+G_y)y+(k_z+G_z)z]} \quad (3)$$

$$\phi_{xz} = \sum_{G_x,G_y} \frac{C_{v,\vec{G}}}{\sqrt{V}} e^{i[(k_x+G_x)x+(k_z+G_z)z]} \quad (4)$$

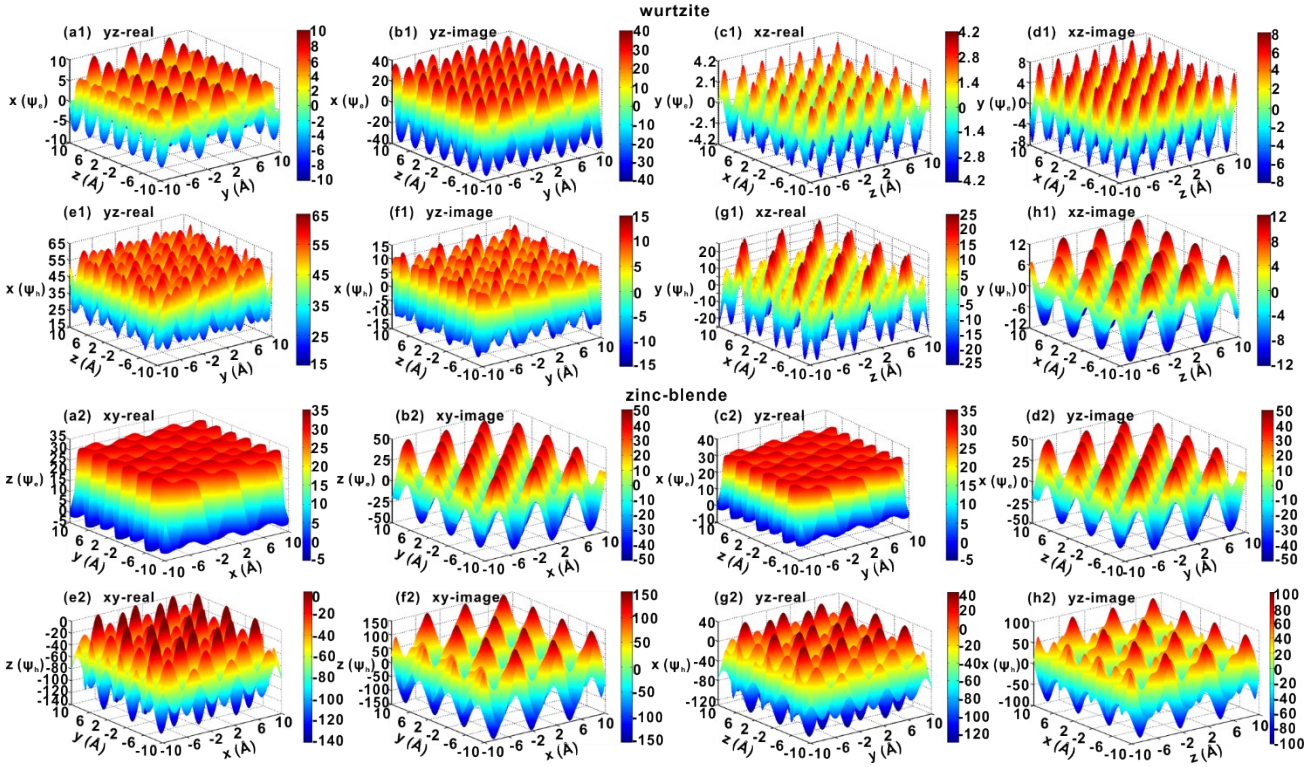

Fig. S6 Electron wave functions Ψ_e of the bottom of conduction band and hole wave functions Ψ_h of the top of the valence band at G point of direct bandgap wurtzite and zinc-blende CdS semiconductors, separately. For wurtzite CdS structures, (a1, e1) the real parts of Ψ_e and Ψ_h wave functions in the yz planes, (b1, f1) the imaginary parts of Ψ_e and Ψ_h wave functions in the yz planes, (c1, g1) the real parts of Ψ_e and Ψ_h wave functions in the xz planes, (d1, h1) the imaginary parts of Ψ_e and Ψ_h wave functions in the xz planes, respectively. For zinc-blende CdS structures, (a2, e2) the real parts of Ψ_e and Ψ_h wave functions in the xy planes, (b2, f2) the imaginary parts of Ψ_e and Ψ_h wave functions in the xy planes, (c2, g2) the real parts of Ψ_e and Ψ_h wave functions in the yz planes, (d2, h2) the imaginary parts of Ψ_e and Ψ_h wave functions in the yz planes, separately.

REFERENCES

1 D. Q. Gao, G. J. Yang, J. Zhang, et al., *Appl. Phys. Lett.*, 2011, **99**, 052502.

2 P. G. Baranov, A. A. Soltamova, D. O. Tolmachev, et al., *Small*, 2011, **7**, 1533-1537.

3 R. M. Feenstra, N. Srivastava, Q. Gao, et al., *Phys. Rev. B*, 2013, **87**, 041406.

4 A. Z. Wang, X. M. Zhang and M. W. Zhao, *Nanoscale*, 2014, **6**, 11157-11162.